Journal of the Serbian Chemical Society
JSCS-info@shd.org.rs • www.shd.org.rs/JSCS
J. Serb. Chem. Soc. *81* (4) 433–446 (2016)
JSCS–4858
UDC 66.017.000.57:543.424.2:535.37+549.753.1–36
Original Scientific paper

Cerium-doped hydroxyapatite nanoparticles synthesized by the co-precipitation method

CARMEN STELUTA CIOBANU[1,2], CRISTINA LIANA POPA[1] and DANIELA PREDOI[1]*

[1]*National Institute of Materials Physics, P. O. Box MG 07, 07725, Magurele, Romania and*
[2]*University Politehnica of Bucharest, Faculty of Applied Chemistry and Materials Science, Department of Science and Engineering of Oxide Materials and Nanomaterials, 1–7 Polizu Street, P. O. Box 12–134, 011061 Bucharest, Romania*

(Received 24 August, revised 20 December, accepted 25 December 2015)

Abstract: The present work reports a simple adapted co-precipitation method for the synthesis of stable Ce-substituted Ca hydroxyapatite (HAp) nanoparticles. The structural and morphological properties of the Ce-doped hydroxyapatite (Ce:HAp) were characterized by X-ray diffraction (XRD), transmission electron microscopy (TEM), scanning electron microscopy (SEM) and energy dispersive X-ray analysis (EDAX). The optical properties of the Ce-doped hydroxyapatite were also investigated using Fourier transform infrared (FTIR) spectroscopy, Fourier transform Raman spectroscopy and photoluminescence analysis. The results of the XRD studies revealed the progressive increase in the *a*- and *c*-axes with increasing Ce concentration. In the FTIR studies of Ce:HAp powders, a structure similar to that of hydroxyapatite was observed. The IR and Raman wavenumbers and the peak strengths of the bands associated with the P–O and O–H bonds decreased progressively with increasing Ce concentration. All the emission maxima could be attributed to 5d–4f transitions of the Ce ions. The displacements of the maximum emission bands with increasing Cerium in the samples were in agreement with the results obtained by XRD studies. The Ce:HAp samples with x_{Ce} = 0.03 and 0.05 exhibited significant antibacterial activity against *Staphylococcus aureus* and *Escherichia coli* bacterial strains compared to Ce:HAp samples with x_{Ce} = 0 (pure HAp) and 0.01.

Keywords: biomaterials; FTIR; FT Raman; photoluminescence; *Staphylococcus aureus*; *Escherichia coli*.

INTRODUCTION

Hydroxyapatite is one of the most studied biomaterial with the chemical formula $Ca_{10}(PO_4)_6(OH)_2$, (HAp) and represents the principal inorganic component

* Corresponding author. E-mail: dpredoi@gmail.com
doi:10.2298/JSC150824007C

of bones and teeth. Its excellent biological properties (biocompatibility, osteoconductivity, inductivity, *etc*.) have made HAp a suitable material for the biomedical field.[1–6] Recent studies demonstrated that the structure of apatite allows a large number of substitutions.[7–9] These substitutions modify the physical, chemical and biological properties of HAp. Moreover, the crystallinity, solubility and thermal stability are also influenced by the substitution of Ca with different ions (Eu, Ag, Sm, Zn, Cu, *etc*.). The substitution of Ca with Ce is also possible because their radius and electronegativity are very similar.

Studies conducted by Doat *et al*. showed that lanthanide-doped hydroxyapatite (*e.g*., europium-doped hydroxyapatite) nanoparticles could be used as bioactive fluorescent carriers of biological molecules and drugs.[10–12]

It is well known that the morphology, structure and physicochemical properties of HAp powders depend on the synthesis method. Thus, various techniques are used to synthesize hydroxyapatite nanopowders, such as precipitation, sol–gel, solid-state reactions, pyrolysis, microwave synthesis, a mechanochemical route.[13–16]

It was found that cerium (Ce) can act similarly to calcium in the human body and accumulate in bones. According to these results, cerium-doped hydroxyapatite could improve/stimulate metabolism.[17,18] On the other hand, cerium ions also have antimicrobial activity and unique regenerative properties. Moreover, recent studies showed that the use of cerium in dentistry may help prevent cavities.[19,20] These biological properties make cerium suitable for applications in the biomedical field.[21]

A large number of studies were also conducted in order to discover new biomaterials with improved biological and physicochemical properties (especially antibacterial and luminescent) in order to be successfully used in the biomedical field.

As Ce cations possess luminescent properties (under UV excitation[22,23]) and antimicrobial activity, their incorporation in the structure of HAp could lead to a biomaterial being obtained with promising applications in medicine (for imaging, drug delivery, *etc*.).[24]

The present structural, morphological and optical studies were conducted on $Ca_{10-x}Ce_x(PO_4)_6(OH)_2$ (Ce:Hap) synthesized by the co-precipitation method. Small concentrations of cerium (x_{Ce} = 0.01, 0.03 and 0.05) were incorporated in the hydroxyapatite structure in order to demonstrate that Ca was replaced by Ce in the apatite lattice. The structural changes to the apatite lattice after Ca substitution by Ce at small concentrations is described herein for the first time. All Ce:HAp samples were characterized by X-ray diffraction (XRD), transmission electron microscopy (TEM), scanning electron microscopy (SEM), energy dispersive X-ray analysis (EDAX), Fourier transform infrared (FTIR) spectroscopy, FT Raman spectroscopy and photoluminescence analysis. This study proposes

various complementary characterization techniques for a general understanding of what occurs in the apatite lattice when Ca is replaced by Ce.

The aim of this work was also to study the influence of cerium on the physicochemical, photoluminescent and antimicrobial properties of hydroxyapatite doped with small concentrations of cerium.

In addition, the results obtained in this study could be of importance for future studies concerning the influence of rare earths on various ceramic materials.

EXPERIMENTAL

Powders preparation

In this work, Ce-doped $Ca_{10}(PO_4)_6(OH)_2$ powders, ($Ca_{10-x}Ce_x(PO_4)_6(OH)_2$; Ce:HAp) with different concentrations of cerium (x_{Ce} = 0.01, 0.03 and 0.05) were synthesized by the co-precipitation method. In order to obtain Ce:HAp powders, appropriate amounts of cerium nitrate hexahydrate $Ce(NO_3)_3{\cdot}6H_2O$ (99.999 %, Sigma–Aldrich) and calcium nitrate tetrahydrate $Ca(NO_3)_2{\cdot}4H_2O$ (99.999 %, Sigma–Aldrich) were dissolved in deionised water, resulting 350 mL of solution (solution 1). In a separate beaker, an appropriate amount of $(NH_4)_2HPO_4$ (≥98 %, Sigma–Aldrich) was dissolved in deionised water, resulting 350 mL of solution (solution 2). Both solutions were obtained under vigorous stirring (300 rpm, 150 °C, 1 h) on a magnetic stirrer (Velp Scientifica). Solution 2 was dropped into solution 1 under vigorous stirring (300 rpm) at 100 °C. The pH of the mixture was adjusted to 10 by the addition of NH_4OH. The resulting precipitate was washed several times with deionised water and then filtered. The powder was dried at 100 °C for 48 h in an air oven.

Powders characterization

The powders were investigated by X-ray diffraction using a Bruker D8 Advance diffractometer, with nickel filtered CuK_α (λ = 1.5418 Å) radiation and a high efficiency one-dimensional detector (Lynx Eye type) operated in the integration mode. The diffraction patterns were collected in the 2θ range 20–60°, with a step of 0.02° and 34 s measuring time per step. Insightful analyses of the Ce:HAp structures were performed by Rietveld refinement analysis using the MAUD code.[25,26] Transmission electron microscopy (TEM) studies were realised using a JEOL 200 CX instrument. Scanning electron microscopy (SEM) measurements were performed using a Quanta Inspect F microscope from the FEI Company, equipped with an energy-dispersive X-ray spectrometer (EDAX). The FTIR studies of the powders were performed on a Spectrum BX Spectrometer using the KBr pellet technique. The spectra were registered in the spectral region 400–4000 cm^{-1} with a resolution 4 cm^{-1} and 128 scans. An FT Raman Bruker RFS 100 spectrophotometer was used in order to obtain complementary information about optical properties of the Ce:HAp powders. The powders were excited using a laser wavelength of 1064 nm. The spectra were recorded with a resolution of 4 cm^{-1} and 100 scans. The fluorescence emission spectra were obtained on a HORIBA Scientific Fluorolog-3 spectrofluorometer (model FL3-2iHR320 with Hamamatsu R-928 PMT).

Antibacterial tests

The antibacterial activity of Ce:HAp samples were investigated against Gram-positive and Gram-negative bacterial strains, *i.e.*, *Staphylococcus aureus* ATCC 6538 and *Escherichia coli* 714. The antibacterial activity was assessed using the standardized Kirby–Bauer disc diffusion method.[27] The *S. aureus* ATCC 6538 and *E. coli* 714 bacterial strains were acquired

from American Type Culture Collection. The Ce:HAp samples were inoculated on Mueller–Hinton agar plates followed by incubation at 37 °C for 24 h. To evaluate the antibacterial activity of the Ce:HAp samples, the inhibition areas were examined. The total diameter (in mm) of the inhibition zone was measured for each sample. The survival rates of the *S. aureus* and *E. coli* bacterial strains were evaluated after they had been exposed to the Ce:HAp and pure HAp (as reference) bioceramic powders. The tests for all Ce:HAp samples were performed in triplicate.

RESULTS AND DISCUSSIONS

The X-ray diffraction patterns of cerium doped hydroxyapatite, $Ca_{10-x}Ce_x(PO_4)_6(OH)_2$, with different concentrations of cerium (x_{Ce} = 0.01, 0.03 and 0.05) are depicted in Fig. 1A. The broad peaks in the X-ray diffraction patterns assigned to the characteristic (002), (210), (211), (300), (202), (310), (222), (123) and (004) planes of $Ca_{10-x}Ce_x(PO_4)_6(OH)_2$ were in accordance with the expected patterns for crystalline hydroxyapatite with a hexagonal structure (JCPDS No. 9-432). Separate phases for cerium oxide or other impurity phases were not observed in these diffraction patterns. Nevertheless, when some Ca sites were replaced by Ce, there was some distortion of the lattice cell parameters. For the peaks registered at lower degrees, a slight shift was observed. This behaviour seems to be the effect of substitutions that change the crystal structure (Fig. 1B), which according to Lim *et al.*[28] suggests a significant incorporation of the dopants into the apatite lattice.

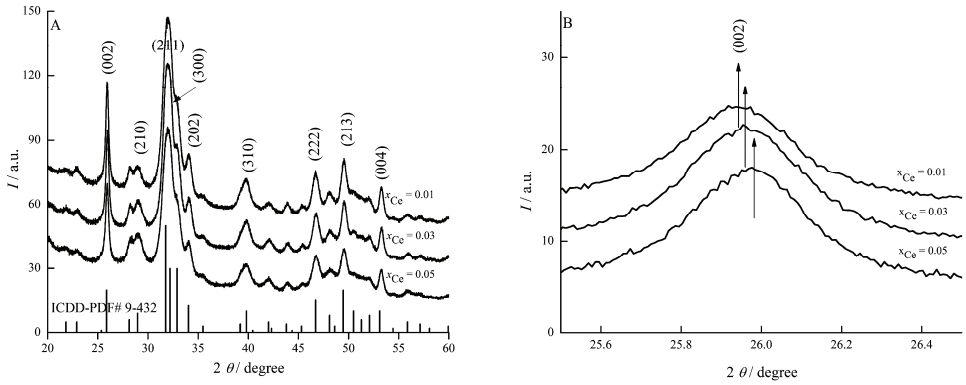

Fig. 1. A) X-ray diffraction patterns of Ce:HAp with x_{Ce} = 0.01, 0.03 and 0.05; B) comparison of the X-ray diffraction patterns for Ce:HAp with x_{Ce} = 0.01, 0.03 and 0.05.

The crystallite sizes of all the Ce:HAp samples decreased with increasing Ce concentration in the samples (Table I). In this study, both the *a*- and *c*-axes increased with increasing Ce substitution (Table I). This result is logical because the ionic radius of Ce (0.107 nm) is greater than that of Ca (0.100 nm) and packaging of the larger size atoms has the tendency to distort the lattice parameters.[29–32]

These results obtained from XRD studies demonstrate that the Ce:HAp powders synthesised by the adapted co-precipitation method revealed the characteristic structure of hydroxyapatite with good crystal structure without the presence of any new phase or impurity.

TABLE I. Lattice cell parameters and the crystallite sizes of $Ca_{10-x}Ce_x(PO_4)_6(OH)_2$ obtained from Rietveld refinement

x_{Ce}	Cell parameters		Crystallite size, nm
	a / nm	c / nm	
(JCPDS 9-432)	0.9418	0.6884	–
0.01	0.9420±0.0001	0.6886±0.0001	25.45±0.1
0.03	0.9424±0.0002	0.6889±0.0003	22.86±0.1
0.05	0.9436±0.0002	0.6895±0.0004	18.95±0.1

In order to examine the microstructure and elemental composition of Ce:HAp powders, scanning electron microscopy studies were performed. The SEM images and EDAX spectra of the Ce:HAp samples are presented in Fig. 2. From the

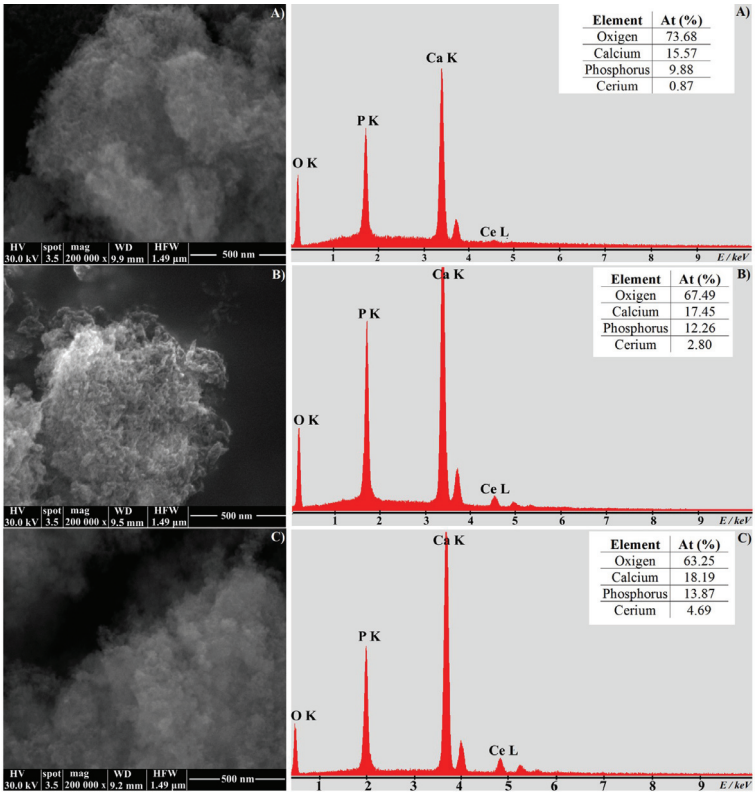

Fig. 2. SEM images and EDAX spectra of Ce:HAp powders (x_{Ce} = 0.01 (A), 0.03 (B) and 0.05 (C)).

SEM images, it could be observed that the increase in the Ce concentration slightly influenced the morphology of the samples. However, the ellipsoidal shape of the nanoparticles was preserved in all the samples. The SEM micrographs confirmed the nanometric dimensions of the particles but also their tendency to agglomerate. This tendency to agglomerate is due most probably to the nanometric dimensions of the particles.

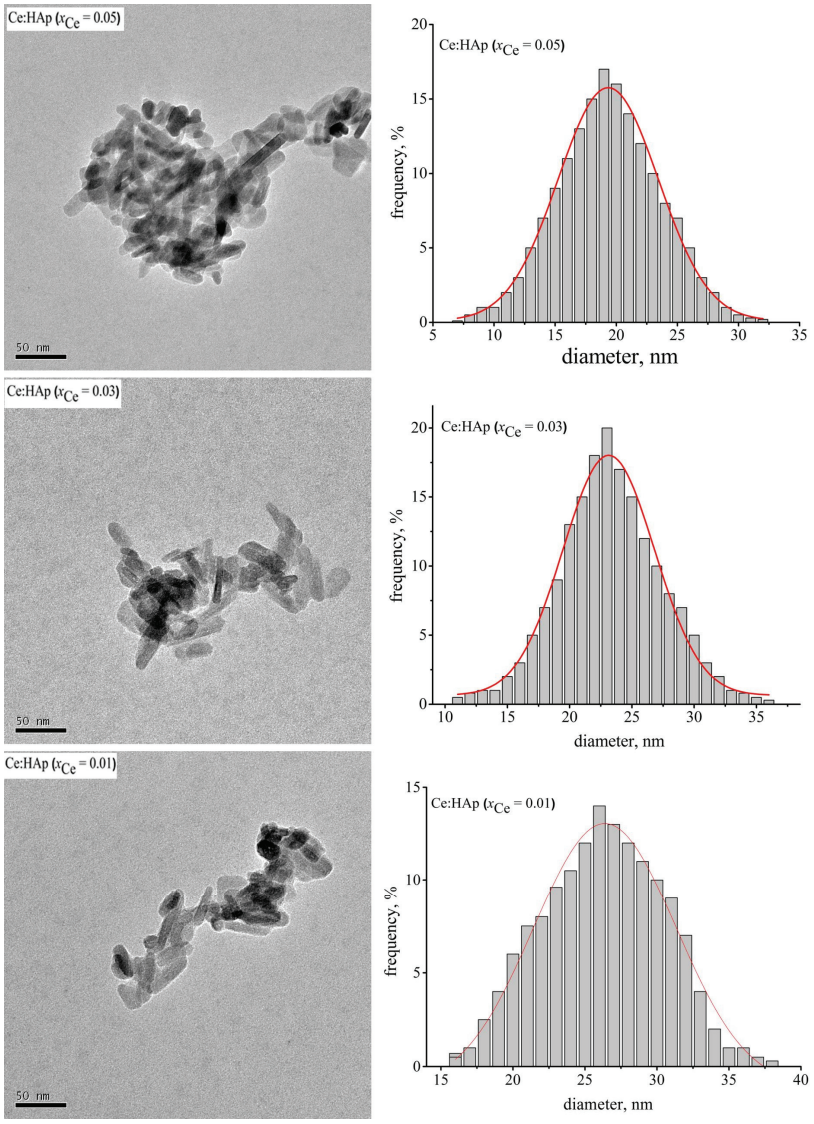

Fig. 3. TEM images and size distribution of Ce:HAp samples (x_{Ce} = 0.01 (A), 0.03 (B) and 0.05 (C)).

The EDAX spectra (Fig. 2b) of the studied powders confirmed the presence of all constituent elements of the Ce:HAp powders: Ce, Ca, P and O. In the tables inserted in the EDAX spectra, the calculated atomic ratios of the constituent elements for each powder are presented. These results suggest that cerium ions were incorporated in the hydroxyapatite structure. Moreover, these studies confirmed the increase of the Ce concentrations in the samples.

The TEM images of the synthesized samples are presented in Fig. 3 (left). The TEM images clearly demonstrated the morphologies of Ce:HAp nanoparticles. The grain size of the Ce:HAp samples determined from TEM images are in full agreement with the results from the XRD studies. The mean particle size was determined from TEM images after counting approximately 500 nanoparticles Fig. 3 (right). Therefore, the average particle size obtained for Ce:HAp with x_{Ce} = 0.01 was 26.5±0.5 nm, for the Ce:HAp powder with x_{Ce} = 0.03, it was 23±0.1 nm and for Ce:HAp with x_{Ce} = 0.05, it was 19.5±0.1 nm.

In the FTIR spectra of cerium doped hydroxyapatite (Fig. 4), characteristic vibrational bands related to phosphate, hydroxyl and adsorbed water were present. Moreover, an additional band attributed to the carbonate group (1269 cm^{-1}) was also presented.

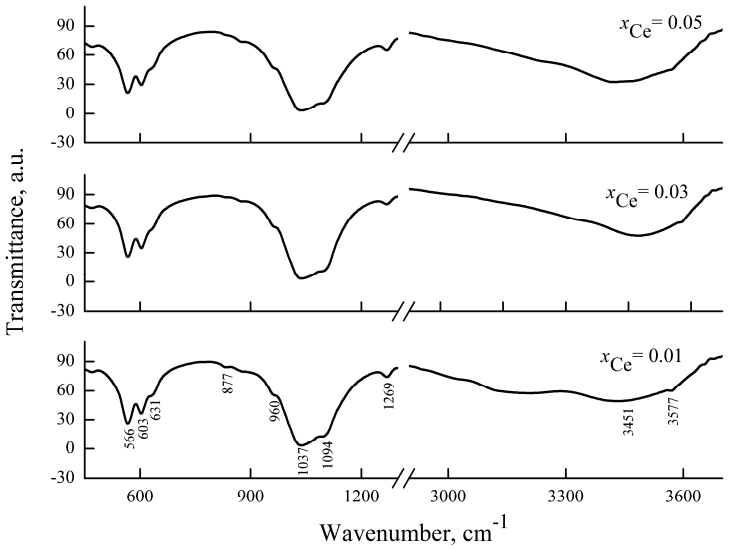

Fig. 4. FTIR spectra of the cerium-doped hydroxyapatite powders.

The vibrational bands from the region 3100–3460 cm^{-1} were attributed to adsorbed water. The bands at 3577 and 631 cm^{-1} were assigned to the stretching and vibrational mode of the hydroxyl group (OH^-).[33–35] The presence of the

bands at 566, 603 (assigned to the ν_4 bending mode of PO_4^{3-} groups) and 631 cm^{-1} indicate the formation of a well crystallized powder.

The phosphate ν_1 stretching mode band was present at 960 cm^{-1} and the PO_4^{3-} ν_3 stretching mode band at 1094 and 1037 cm^{-1}. Furthermore, the band at 470 cm^{-1} was assigned to the ν_2 bending mode band of the PO_4^{3-} group. In addition, the IR wavenumber and the peak strength of the P–O and O–H bonds decreased progressively with increasing Ce concentration.

Complementary information to those obtained by FTIR spectroscopy was obtained by Raman spectroscopy. The main vibrational bands observed in the Raman spectra (Fig. 5) were attributed to the stretching (ν_3 and ν_1) and bending (ν_4) modes of the phosphate group from the HAp structure. The bands from 594 and 610 cm^{-1} were assigned to the ν_4 bending mode of the PO_4^{3-} group. On the other hand, the phosphate ν_1 stretching mode band appeared at 965 cm^{-1} and another stretching mode (ν_3) was observed at 1053 cm^{-1}.

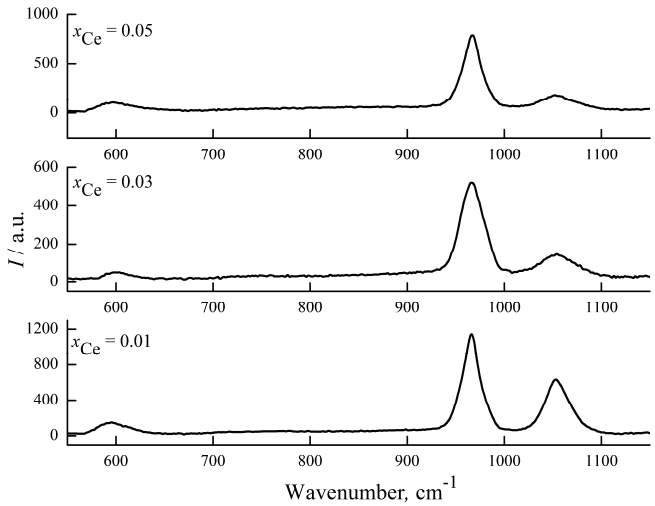

Fig. 5. Raman spectra of cerium-doped hydroxyapatite powders.

In the Raman spectra we could also observe that the intensity of the vibrational bands decreased with the increase of Cerium concentration in the powders. This behaviour is due to the substitution of Ca ions with larger ions (Ce) in the HAp lattice which leads to a decrease of bonding strength of P–O.[23] These results obtained by Raman spectroscopy are in good agreement with the information derived from the FTIR studies presented above. On the other hand, the results obtained by FTIR and Raman spectroscopy confirmed the XRD analysis.

The emission spectra of Ce:HAp samples with x_{Ce} = 0.01; 0.03 and 0.05 are presented in Fig. 6. Under an excitation of 250 nm, the spectrum had a maximum

at around 390 nm and a shoulder at about 350 nm that covered the wavelength range from 330 to 430 nm.

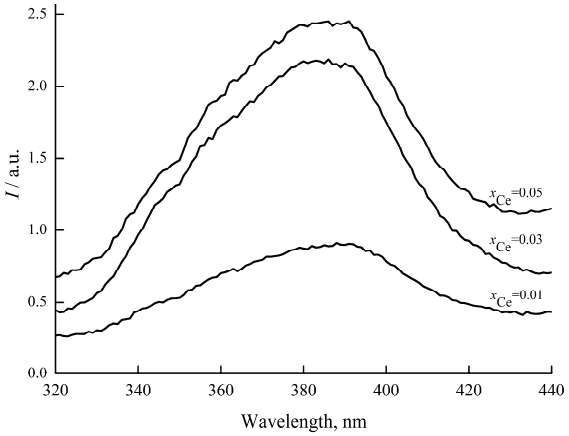

Fig. 6. Emission spectra of Ce:HAp powders (x_{Ce} = 0.01, 0.03 and 0.05); λ_{exc} = 250 nm.

As the spectra were asymmetric, they were deconvoluted into four Gaussian peaks with maxima at around 390, 375, 357 and 347 nm (Fig. 7). All these emission maxima could be attributed to 5d–4f transitions of the Ce ions.

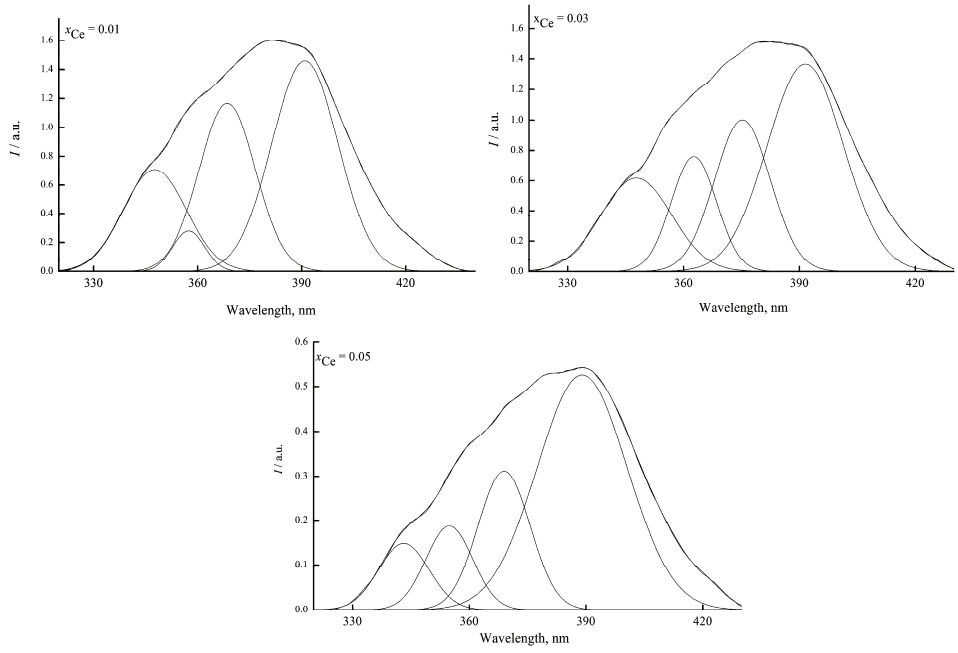

Fig. 7. Deconvolution of the emission spectra of Ce:HAp powders (x_{Ce} = 0.01; 0.03 and 0.05); λ_{exc} = 250 nm.

In the structure of HAp two types of Ca site (positions) are present: Ca (I) and Ca (II). Here, the emission maximum around 360 nm is attributed to Ce ion which substituted the Ca(I) position in the hydroxyapatite structure.[36] In addition, the emission band at around 390 nm occurred due to Ce ion that substituted the Ca(II) position. The results reported in this paper are in good agreement with data reported in the literature.[36] Furthermore, it is obvious that the intensity of the emissions bands increased with increasing cerium concentrations in the samples. Furthermore, the maximum emission bands were displaced with increasing cerium in the samples. These results are in agreement with the results obtained by XRD studies.

The antimicrobial activity of the cerium substituted hydroxyapatite against *E. coli* 714 and *S. aureus* ATCC 6538 bacteria was studied after 24 h incubation (Figs. 8 and 9, respectively). The antimicrobial activity of the cerium-substituted hydroxyapatite was compared with that of pure hydroxyapatite ($x_{Ce} = 0$), which was considered as the reference. According to a previous study,[37] pure HAp did not exhibit any antibacterial effect against *E. coli* 714 and *S. aureus* ATCC 6538. The results of this study suggest that the survival rate of *E. coli* 714 bacterial strain decreased with increasing concentration of Ce in the hydroxyapatite. Moreover, for $x_{Ce} = 0.05$, the antibacterial effect against *E. coli* 714 was significant (*$p < 0.05$, compared to pure HAp).

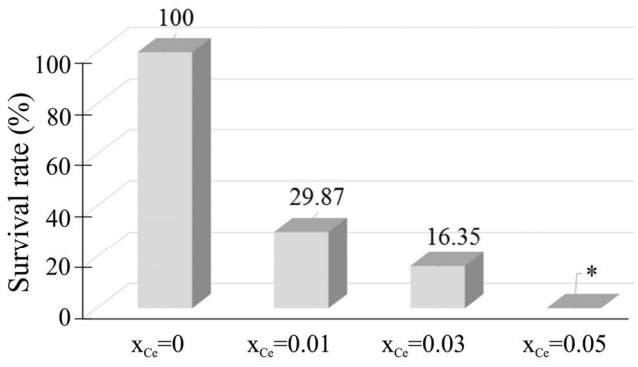

Fig. 8. The survival rate of *E. coli* 714 in dependence on the concentration of Ce in the analyzed samples; *$p < 0.05$.

The survival rate of *S. aureus* in dependence on the concentration of Ce in the analyzed samples is presented in Fig. 9. The survival rate of the *S. aureus* ATCC 6538 bacterial strain decreased with increasing concentration of Ce in the hydroxyapatite. However, the survival rate of *S. aureus* ATCC 6538 was still around 10 % when $x_{Ce} = 0.05$. To demonstrate that the antimicrobial effect of Ce:HAp was greater against Gram-

-negative bacteria than Gram-positive bacteria, future studies on the effect against several strains of Gram-positive and Gram-negative are required.

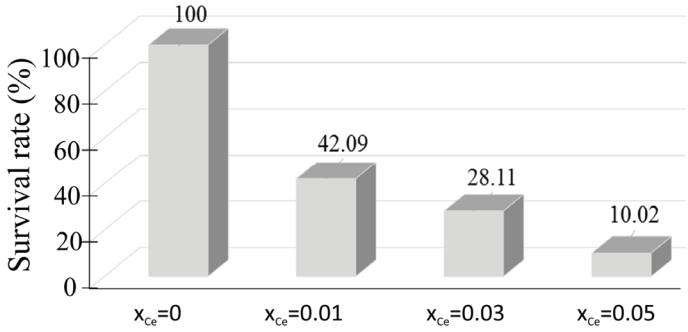

Fig. 9. The survival rate of *S. aureus* ATCC 6538 in dependence on the concentration of Ce in the analyzed samples.

The results of this research demonstrated that cerium-doped hydroxyapatite may be prepared by the co-precipitation method at low temperatures. Ce^{3+} can enter into the HAp structure by substituting calcium ions. After substituting Ca^{2+} in hydroxyapatite structure, the crystallite sizes of Ce:HAp decreased with increasing cerium concentration. According to previous studies,[38] the crystallinity decreased gradually with increasing cerium concentration in the Ce:HAp samples. Many studies have been focused on the synthesis of various materials based on rare earth elements with antimicrobial activity and their applications in different biological fields was highlighted.[39]

The antimicrobial activity of the cerium-substituted hydroxyapatite with low concentrations of cerium was compared to that of pure HAp. The antimicrobial activities of pure HAp against *E. coli* 714 and *S. aureus* ATCC 6538 were comparable with previous results.[8,9] On the other hand, the present study demonstrated that the antimicrobial activities of hydroxyapatite doped with low concentrations of cerium against *E. coli* 714 and *S. aureus* ATCC 6538 were more pronounced than those reported in previous studies for copper-doped hydroxyapatite.[40] In addition, the present study also showed that the antimicrobial activity of cerium-substituted hydroxyapatite was more pronounced than the antimicrobial activity of both unsubstituted hydroxyapatite and fluorapatite.[41,42] This result could be explained by the interaction of cerium ions present in the hydroxyapatite structure with the cell membrane that could lead to structural damage and death of the cells.[43,44] This research demonstrated that cerium is a good candidate that could impart excellent antibacterial activity on HAp.

CONCLUSIONS

In this article, the synthesis of hydroxyapatite doped with small concentration of cerium is reported. The lattice parameters showed that Ce substituted Ca in the apatite structure. The crystal size decreased with increasing concentration of Ce. The results obtained in the XRD studies demonstrated that the Ce:HAp powders synthesized by an adapted co-precipitation method gave hydroxyapatite with a good crystalline structure without any new phases or impurities. The nanometric dimensions of the particles were confirmed by SEM and TEM micrographs. Raman and FTIR studies confirmed the initial results obtained by XRD investigations. The deconvolution of the emission spectra of all Ce:HAp samples revealed four peaks that could be attributed to 5d–4f transitions of the Ce ions. This research demonstrated that cerium is a good candidate that can provide HAp an excellent antibacterial activity. In conclusion, the results presented in this paper encourage further studies and research on the antimicrobial properties of cerium-doped hydroxyapatite aimed at possible applications as an antimicrobial agent.

Acknowledgements. The work was funded by the Sectoral Operational Programme Human Resources Development 2007–2013 of the Ministry of European Funds through the Financial Agreement POSDRU/159/1.5/S/134398. We thank HORIBA Scientific and especially Dr. Reynald Hurteaux and Dr. Patrick Chapon from Horiba Jobin Yvon SAS France for the access to their specific instrumentation.

ИЗВОД

ЦЕРИЈУМОМ ДОПИРАНЕ НАНОЧЕСТИЦЕ ХИДРОКСИАПАТИТА СИНТЕТИСАНЕ МЕТОДОМ КОПРЕЦИПИТАЦИЈЕ

CARMEN STELUTA CIOBANU[1,2], CRISTINA LIANA POPA[1] и DANIELA PREDOI[1]

[1]*National Institute of Materials Physics, P.O. Box MG 07, 07725, Magurele, Romania* и [2]*University Politehnica of Bucharest, Faculty of Applied Chemistry and Materials Science, Department of Science and Engineering of Oxide Materials and Nanomaterials, 1–7 Polizu Street, P.O. Box 12–134, 011061 Bucharest, Romania*

У раду је приказан једноставни модификовани копреципитациони поступак за синтезу стабилних Се-допираних наночестица Са-хидроксиапатита (HAp). Структурна и морфолошка својства синтетисаних прахова Се:HAp су испитивана применом рендгенске дифракционе анализе (XRD), трансмисионе електронске микроскопије (TEM), скенирајуће електронске микроскопије (SEM) и енергетске дисперзивне спектроскопије (EDS). Оптичка својства Се-допираних хидроксиапатита су испитивана применом инфрацрвене спектроскопије са Фуријеовим трансформацијама (FTIR), Раман спектроскопије са Фуријеовим трансформацијама и фотолуминисцентном анализом. Резултати XRD анализе су показали да долази до континуалног повећања *a* и *c* параметара јединичне ћелије са повећањем концентрације церијума. FTIR анализа прахова Се:HAp је показала сличну структуру добијених прахова. IR и Раман таласни бројеви, као и интензитети трака које одговарају везама P–O и O–H опадају континуално са повећањем концентрације Се. Сви емисиони максимуми могу се приписати 5d–4f прелазу Се-јона. Померање емисионих максимума са повећањем концентрације церијума у узорцима је у

сагласности са резултатима XRD анализе. Ce:HAp узорци са x_{Ce} = 0,03 и 0,05 показују значајно већу антибактеријску активност према бактеријским врстама *Staphylococcus aureus* ATCC 6538 и *Escherichia coli* 714 у односу на узорак Ce:HAp са x_{Ce} = 0 (чист HAp) и x_{Ce} = 0,01.

(Примљено 24. августа, ревидирано 20. децембра, прихваћено 25. децембра 2015)

REFERENCES

1. R. Gorcia, R. H. Doremus, *J. Mater. Sci. – Mater. Med*. **3** (1992) 154
2. C. K. Hsu, *Mater. Chem. Phys.* **9470** (2002) 1
3. T. Kokubo, *Bioceramics and their Clinical Applications,* CRC Press, Boca Raton, FL, 2008
4. J. Park, *Bioceramics: Properties, Characterizations and Applications*, Springer, New York, USA, 2008, p. 359
5. S. V. Dorozhkin, *Calcium orthophosphates: applications in nature, biology and medicine,* Pan Stanford, Singapore, 2012, p. 850
6. S. V. Dorozhkin, *J. Mater. Sci. – Mater. Med.* **24** (2013) 1335
7. C. S. Ciobanu, C. L. Popa, D. Predoi, *J. Nanomat.* **2014** (2014) 1
8. C. S. Ciobanu, F. Massuyeau, L. V. Constantin, D. Predoi, *Nanoscale Res. Lett.* **6** (2011) 613
9. C. S. Ciobanu, S. L. Iconaru, F. Massuyeau, L. V. Constantin, A. Costescu, D. Predoi, *J. Nanomater.* **2012** (2012) 1
10. S. P. Mondejar, A. Kovtun, M. Epple, *J. Mater. Chem.* **17** (2007) 4153
11. P. Yang, Z. Quan, C. Li, X. Kang, H. Lian, J. Lin, *Biomaterials* **29** (2008) 4341
12. A. Doat, F. Pellé, N. Gardant, A. Lebugle, *J. Solid State Chem.* **177** (2004) 1179
13. S. Koutsopoulos, *J. Biomed. Mater. Res.* **62** (2002) 600
14. S. V. Dorozhkin, *Int. J. Chem. Mater. Sci.* **1** (2013) 105
15. M. S. Djošić, M. Mitrić, V. B. Mišković-Stanković, *J. Serb. Chem. Soc.* **80** (2015) 237
16. A. Janković, S. Eraković, A. Dindune, D. Veljović, T. Stevanović, D. Janaćković, V. Mišković-Stanković, *J. Serb. Chem. Soc.* **77** (2012) 1609
17. J. Emsley, *Nature's Building Blocks: An A–Z Guide to the Elements*, Oxford University Press, Oxford, 2011
18. M. A. Jakupec, P. Unfried, B. K. Keppler, *Rev. Physiol. Biochem. Pharmacol.* **153** (2005) 101
19. J. Kiss, J. Bánóczy, E. Fehérváry, Z. Gintner, M. Albrecht, *Acta Morphol Hung*. **38** (1990) 61
20. X. F. Liu, M. J. Tu, *Modern Chemical Industry* **25** (2005) 145
21. Y. Lin, Z. Yang, J. Cheng, *J. Rare Earths.* **25** (2007) 452
22. Z. Feng, Y. Liao, M. Ye, *J. Mater. Sci. - Mater. Med.* **16** (2005) 417
23. L. Yingguang, Y. Zhuoru, C. Jiang, *J. Rare Earth.* **25** (2007) 452
24. Ž. Radovanović, Đ. Veljović, B. Jokić, S. Dimitrijević, G. Bogdanović, V. Kojić, R. Petrović, D. Janaćković, *J. Serb. Chem. Soc.* **77** (2012) 1787
25. L. Lutterotti, *Nucl. Instr. Meth. Phys. Res.* **268** (2010) 334
26. N. C. Popa, *J. Appl. Crystallogr.* **31** (1998) 176
27. A. W. Bauer, W. M. Kirby, J. C. Sherris, M. Truck, *Am. J. Clin. Pathol.* **45** (1966) 493
28. P. N. Lim, B. Y. Tay, C. M. Chan, E. S. Thian, *J. Biomed. Mater. Res., B* **100** (2012) 285
29. C. Ergun, T. J. Webster, R. Bizios, R. H. *J. Biomed. Mater Res.* **59** (2002) 169
30. F. Miyaji, Y. Kono, Y. Suyama, *Mater. Res. Bull.* **40** (2005) 209
31. X. L. Tang, X. F. Xiao, R. F. Liu, *Mater. Lett.* **59** (2005) 3841

32. O. Kaygili, S. V. Dorozhkin, S. Keser, *Mat. Sci. Eng., C* **42** (2014) 78
33. I. V. Berezovskaya, N. P. Efryushina, G. B. Stryganyuk, A. S. Voloshinovskii, E. V. Zubar, V. P. Dotsenko, *Func. Mater.* **15** (2008) 164
34. A. Groza, A. Surmeian, *J. Nanomater.* **2015** (2015) 1
35. A. Groza, *Rom. Rep. Phys.* **64** (2012) 1227
36. I. V. Berezovskaya, N. P. Efryushina, E. V. Zubar, V. P. Dotsenko, in *Proceedings of the International Conference Nanomaterials: Applications and Properties*, Sumy State University, Ukraine, 2012, Abstract No. 01PCN24
37. G. Dai, A. Yu, X. Cai, Q. Shi, Y. Ouyang, S. Tan, *J. Rare Earth* **30** (2012) 820
38. L. Yingguang, Y. Zhuoru, C. Jiang, *J. Rare Earth* **25** (2007) 452
39. T. S. H. Perera, Y. Han, X. Lu, X. Wang, H. Dai, S. Li, *J. Nanomater.* **2015** (2015) 1
40. S. Shanmugamn, B. Gopal, *Ceram. Int.* **40** (2014) 15655
41. M. Turkoza, A. Atillab, Z. Evis, *Ceram. Int.* **39** (2013) 8925
42. V. Stanic, S. Dimitrijevic, D. G. Antonovic, B. M. Jokic, S. P. Zeca, S. T. Tanaskovic, S. Raicevi, *Appl. Surf. Sci.* **290** (2014) 346
43. W. L. Du, Y. L. Xu, Z. R. Xu, C. L. Fan, *Nanotechnology* **19** (2008) 085707
44. L. Nan, Y. Liu, M. Lu, K. Yang, *J. Mater. Sci. – Mater. Med.* **19** (2008) 3057.